JOURNAL OF MATERIALS SCIENCE 24 (1989) 3904–3912

Structure of martensite formed in Cu–Al–Fe single crystals during *in situ* HVEM pseudoelastic tensile experiment

J. DUTKIEWICZ
Institute for Metal Research, Polish Academy of Sciences, Kraków, Poland

V. V. MARTYNOV
Institute of Physics of Metals, Academy of Sciences, USSR, Kiev, USSR

U. MESSERSCHMIDT
Institute of Solid State Physics and Electron Microscopy, Academy of Sciences GDR, Halle, GDR

Single crystals of the CuAlFe alloy, containing 14.5 wt% Al and 2.2 wt% Fe were subjected to *in situ* tensile experiment using straining attachment in a 1 MV electron microscope. Load–elongation curves were obtained for three foil plane/tensile direction orientations: (0 0 1) [0 1 0], (0 0 1) [1 1 0] and (1 1 0) [$\bar{1}$ 1 2]. Each crystal was subjected to two cycles of pseudoelastic deformation up to maximum 2% strain, showing almost complete shape recovery. Structure observations and electron diffraction pattern indicated that during deformation of samples of (0 0 1) [1 1 0] and (1 1 0) [1 1 2] orientations, formation of γ_1' martensite was observed and only at later stages narrow needles of β_1' nucleate in front of γ_1'. During pseudoelastic deformation in the (0 0 1) [1 0 0] direction, martensite forms as a mixture of narrow plates possessing either 2H or 18R structures. The following crystallographic relationship between the parent phase and both types of martensite was observed: $[1\,0\,0]\beta_1 \parallel [1\,0\,1]\gamma_1'$ and $(0\,0\,1)\beta_1 \parallel (0\,1\,0)\gamma_1'$; $(0\,0\,1)\beta_1 \parallel (0\,1\,0)\beta_1'$ and $[1\,1\,0]\beta_1 \parallel [0\,0\,1]\beta_1'$. From the character of sidebands reflections presence of $\langle 1\,0\,1\rangle$ $\langle 1\,0\,\bar{1}\rangle$ static displacement waves was inferred.

1. Introduction

Martensite crystals formed during pseudoelastic deformation grow or diminish depending on the driving force of the transformation, preserving coherency with a parent phase [1]. Thermoelastic equilibrium was reported first in CuAlNi alloys [2]. In order to explain the structure changes during pseudoelastic deformation a number of investigations were performed using single crystalline specimen [3–9]. It was shown that external stress not only shifts the characteristic transformation temperature, but also leads to formation of a new martensitic crystal structure. As shown in a CuAl alloy containing more than 13.3% Al [4], cooling leads to formation of 2H-γ_1' martensite, while under an applied stress 9R-β_1' martensite forms, which transforms then into 3R-α_1' fcc. A detailed X-ray study of structures induced by stress in CuAlNi alloys [5] has shown a significant dependence of the structures of martensite on the orientation of the tensile axis in single crystalline specimens. Straining curves show characteristic stages where deformation occurs at a nearly constant stress corresponding to the different martensitic structures. During pseudoelastic deformation of crystals in the [1 1 0] direction only formation of γ_1'-(2H) martensite was reported, while at the [1 0 0] direction β_1'-(9R) martensite forms in the first stage and α_1'(3R) in the second one. When the tensile axis was chosen between both directions then mixed structures were formed. Similar observations were reported in CuAlFe alloys [6], where during deformation in [1 0 0] direction the following sequence of martensitic phases formation was reported:

$$\beta_1 \rightarrow \gamma_1' + \beta_1', \quad \text{then } \gamma_1' \rightarrow \beta_1'', \quad \text{then } \beta_1' + \beta_1'' \rightarrow \alpha_1'.$$

During unloading the phases disappeared in the reverse order.

The structure analysis during tensile experiments was performed in the majority of the previous works [1–6] by means of X-ray diffraction. In our previous paper [7] *in situ* HVEM straining experiments were carried out on CuAlFe single crystals having (0 0 1) foil plane and $\langle 1\,1\,0\rangle$ tensile axis orientation, only 2H-γ_1' martensite was observed.

In the present paper three different crystal orientations were chosen for *in situ* straining experiment in order to show differences in morphology and crystal structure of martensite formed at various orientations of the straining axis.

2. Experimental procedure

Single crystals from a copper alloy containing 14.5 wt% Al and 2.2 wt% Fe were cut into sheets

0022–2461/89 $03.00 + .12

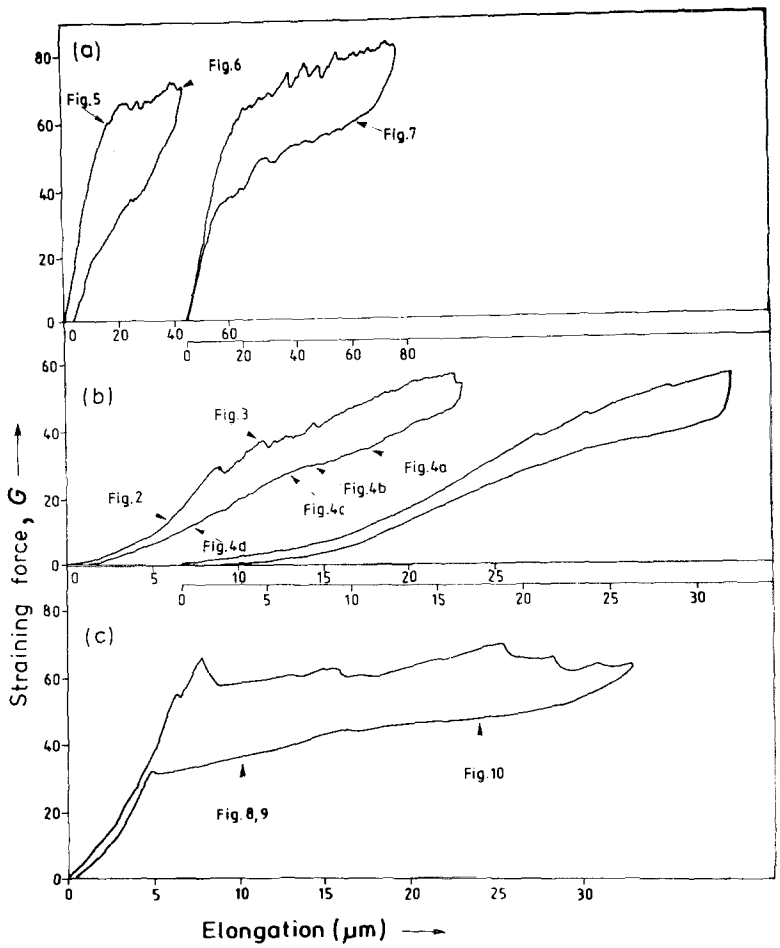

Figure 1 In situ load–elongation curves obtained from single crystals at various orientations: (a) (0 0 1) [0 1 0] two cycles, (b) (0 0 1) [1 1 0] first two cycles, (c) (1 $\bar{1}$ 0) [$\bar{1}$ 1 2] second cycle.

about 1.0 mm thick parallel to $\{1\,1\,0\}$ and $\{0\,0\,1\}$ β_1 planes. The sheets were ground down to 0.2 mm, then chemically polished down to 0.05 mm, and electropolished using a "window" method in an electrolyte consisting of $1/3HNO_3 + 2/3CH_3OH$ at $-40°C$ and a voltage of 10 V, in such a way that thin specimens elongated in the desired direction were obtained. JEOL 1 MV electron microscope equipped with straining attachment described in detail in [10] allowed a maximum elongation of 32 μm corresponding to about 2% of uniform deformation.

3. Results

Figure 1 shows a set of load–elongation curves obtained from single crystals with different foil plane orientation strained *in situ* in the electron microscope at various directions: (a) (0 0 1) [0 1 0], (b) (0 0 1) [1 1 0], and (c) (1 $\bar{1}$ 0) [$\bar{1}$ 1 2] (in this case only the second curve is shown due to recording perturbations in the first cycle). All curves show almost complete shape recovery in the first and the second cycle, although cracks were observed at higher elongations. Curves (a) and (c) have a similar character, i.e. transformation starts at a certain strain and afterwards very low hardening occurs with increasing strain. Curves in Fig. 1b for $\langle 1\,1\,0\rangle$ tensile axis direction differ from those at (a) and (c) and from the one presented in [7]. The main reason is most probably a strong inhomogeneity of deformation due to a specific nonuniform cross section of foil, obtained during thinning.

Figure 2 shows a needle of martensite formed at the [1 1 0] straining direction in the first tensile test. It can be seen that the needle has formed nearly parallel to the tensile direction, while tracks of stacking faults are exactly perpendicular to it. As follows from the diffraction pattern (Fig. 2b) taken from the needle it possesses 2H structure at a [0 1 0] zone axis orientation with the *c*-axis parallel to the tensile direction, and *a*-axis in the plane of the foil. It corresponds to one of the orientation variants observed previously in [5] during deformation in the $\langle 1\,1\,0\rangle$ direction, however one would expect the *a*-axis parallel to the tensile axis due to a slightly higher elongation of this axis during transformation. At higher magnification (Fig. 2c) stacking faults can be clearly seen within the martensite. They form ledges at the β_1–γ_1' phase boundary what may indicate their role in the growth mechanism.

The next micrograph taken at a higher strain (Fig. 3) shows a large area of 2H martensite and a needle that has appeared in front of it in the perpendicular direction to the tensile axis. The diffraction pattern taken from this needle indicates that it possesses the 18R structure with the *c*-axis parallel to the needle. The unexpected formation of 18R martensite at this tensile axis orientation [6, 7] is most probably due to a local strain field in the front of the 2H martensite which favoured the formation of a small needle of the 18R structure.

Figure 4 shows a set of transmission electron micrographs taken with decreasing strain corresponding to

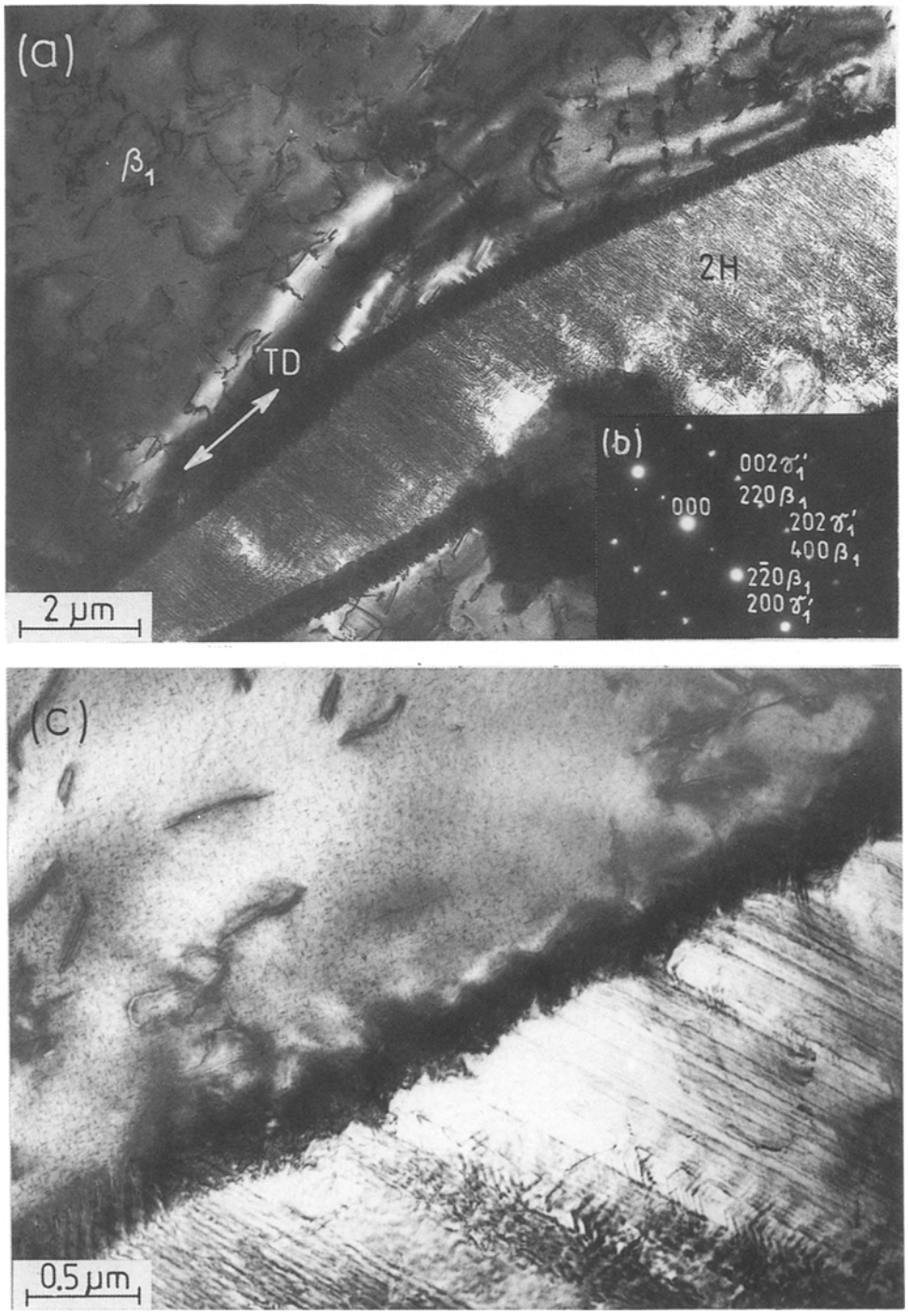

Figure 2 Transmission electron micrographs taken at the initial stage of a load increase in [1 1 0] direction: (a) 2H martensitic needle within β_1 matrix, (b) electron diffraction pattern, (c) martensite interface at higher magnification.

the reverse transformation at points marked in Fig. 1b. A decrease of the area of the 2H martensite can be seen on the following micrographs corresponding to the lower stress. The diffraction pattern (Fig. 4d) taken from the parent phase retransformed from martensite shows diffused streaks in $\langle 1\,1\,0 \rangle$ directions and weak satellites in $\langle 1\,0\,0 \rangle$ directions. The β_1 phase shows a characteristic contrast due to defects left after the reverse transformation.

Observations of structure changes during the tensile test in the [0 0 1] direction suggest a different mechanism of martensite propagation. As can be seen in Fig. 5, martensite grows in the form of closely situated parallel needles. With increasing strain the needles grow in size and new ones appear in the vicinity. As follows from the diffraction pattern (Fig. 5b and d), at the initial stage only needles of the 18R structure are formed, while at a higher deformation the diffraction pattern also shows the presence of 2H martensite. The corresponding micrograph (Fig. 5c) shows on the left side darker narrow needles formed in the later stage that are most probably of the 2H structure.

Figure 6 presents a micrograph taken at the maximum strain during the first cycle. A relatively broad lens-shaped needle of 18R martensite is imaged. Its diffraction pattern (Fig. 6b) consists only of diffraction spots originating from this structure at [0 1 0] orientation. The growth direction is perpendicular to the c-axis of the 18R structure.

The micrograph of Fig. 7 is taken at the beginning

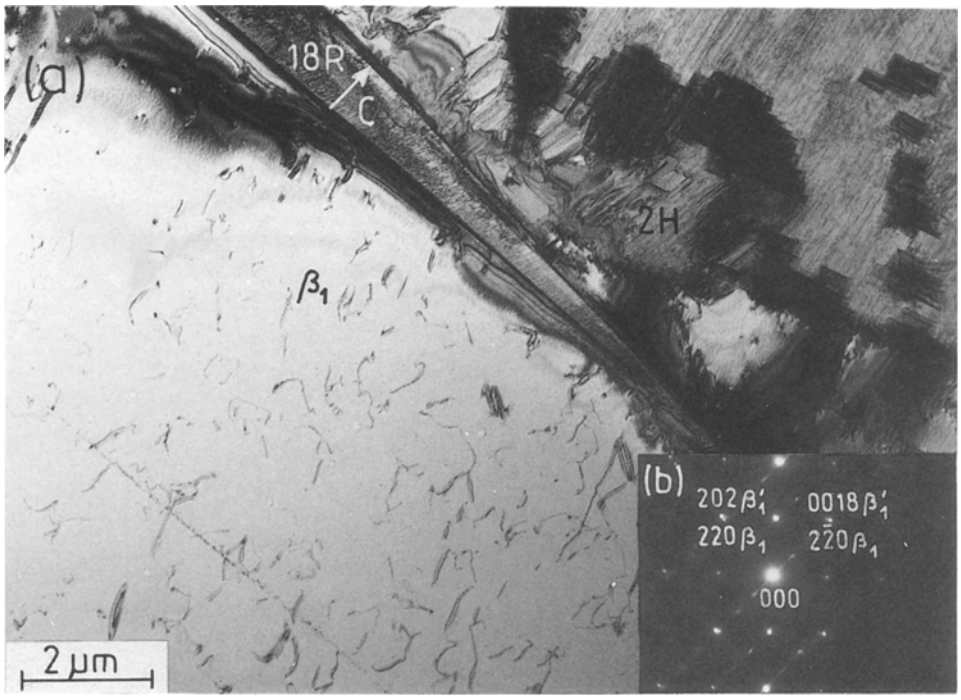

Figure 3 Transmission electron micrograph taken at further stage of load increase in [1 1 0] direction: (a) β_1'-18R martensite needle in front of 2H martensite, (b) electron diffraction pattern.

of the unloading during the second cycle and shows the martensite–matrix phase boundary. It does not exhibit a clear contrast at an orientation close to the symmetrical one. One of reasons for this is that the disappearing needles leave a fringe contrast within the β_1 phase. A diffraction pattern taken from the area of the martensite indicates the presence of 18R and 2H reflections (Fig. 7b). This phenomenon can be explained (similar to the case presented in Fig. 5) by a formation of stress conditions promoting the nucleation of 2H martensite. The diffraction pattern taken from the β_1 area (Fig. 7c) shows diffuse streaks in $\langle 1\,1\,0 \rangle$ directions as in the as-quenched sample and splitting of reflections in $\langle 1\,0\,0 \rangle$ directions due to presence of modulations. The latter effect is much stronger in places where a reverse transformation took place.

A straining experiment was also performed on foils of (1 1 0) orientation in [1 $\bar{1}$ 2] direction. Figure 8 shows a diffraction pattern taken from the sample in the initial stage with strong $\{1\,1\,1\}$ superlattice reflections due to the DO_3 superlattice. In Fig. 9 a parent phase–martensite phase boundary taken at a considerable strain is presented. The diffraction pattern (Fig. 9b) from the central area visible in Fig. 9a shows a set of diffraction spots from martensite and weak reflections

Figure 4 Set of transmission electron micrographs taken with decreasing strain (see Fig. 1) corresponding to decreasing of the 2H martensite area: (a) electron diffraction pattern from the β_1 are shown in (c).

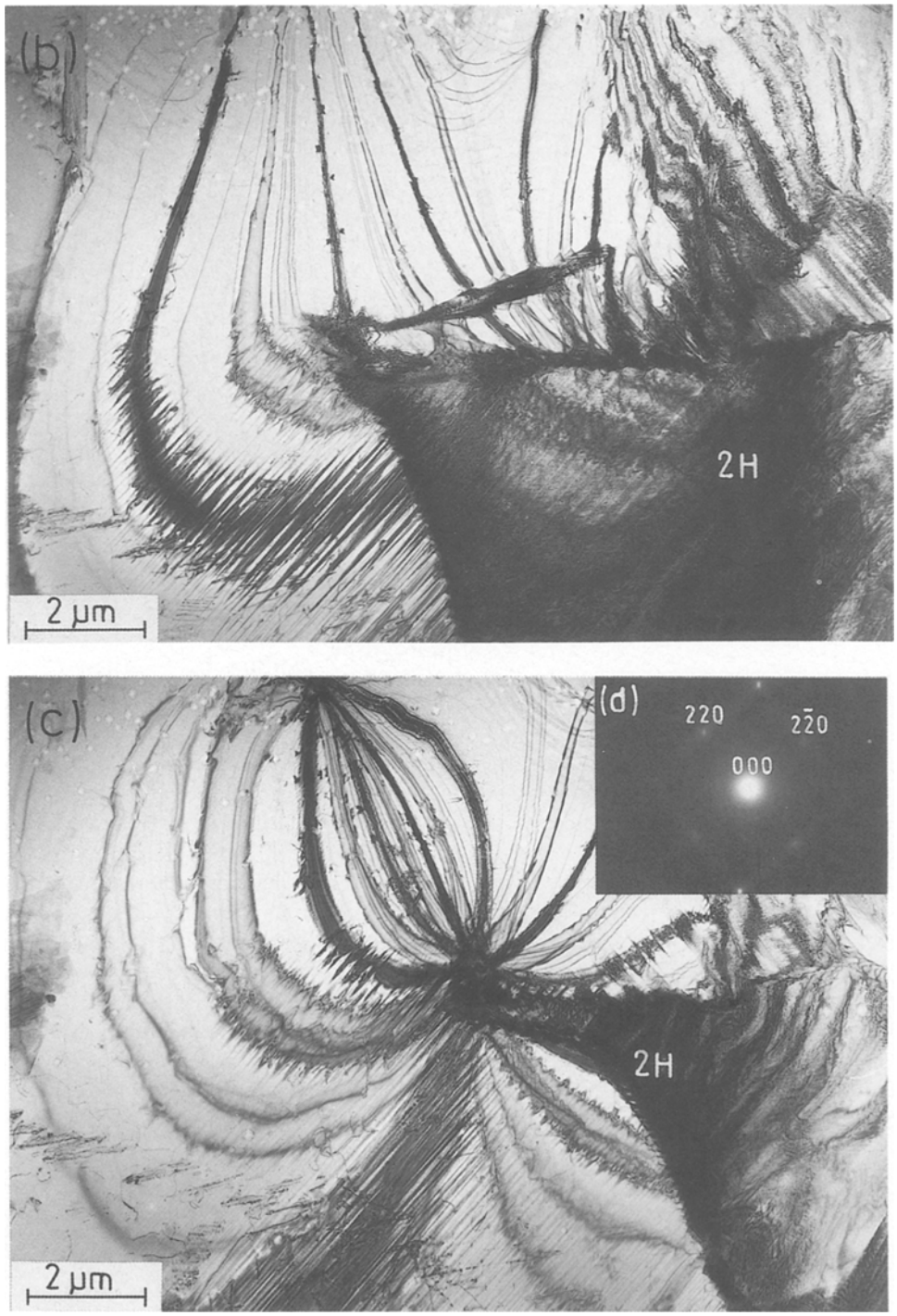

Figure 4 Continued

from the β_1 phase. As results from the indexing the [1 2 $\bar{2}$] zone axis (in hexagonal notation) is parallel to the [0 1 1]β_1, and (1 1 · 0)$\gamma_1' \parallel$ (1 1 1)β_1. Further straining causes the formation of other variants of γ_1' martensite (Fig. 10).

4. Discussion

The present investigation by *in situ* transmission electron microscopy used a different method of sample preparation as compared to previous experiments [3–6, 8, 9]. The maximum uniform tensile strain was limited to about 2%, however due to the nonhomogenity of deformation, even at such low strains cracks were observed at the edge of the specimens. Due to the strain limitation only the parent phase → martensite transformation could be studied and the other ones reported at higher strains, like: $\gamma_1' \rightarrow \beta_1'$ or $\beta_1' \rightarrow \alpha_1'$ [4–6], could not be investigated. Furthermore, due to the irregular shape of the specimen edges one could expect a locally nonuniform stress field. Nevertheless, the character of the tensile curves obtained *in situ* is similar to that reported from bulk specimens [6].

The structure analysis of the pseudoelastic formation of martensite based on electron diffraction confirmed generally the results of former X-ray investigations on CuAlFe [6] and CuAlNi [6, 8] alloys. In the case of the [1 0 0] tensile axis, indeed both martensite phases γ_1' and β_1' were observed during the *in situ* experiment, however, at a [1 1 0] tensile axis β_1' martensite was observed already in the first deformation stage in contrast to X-ray results [6]. This phenomenon can be

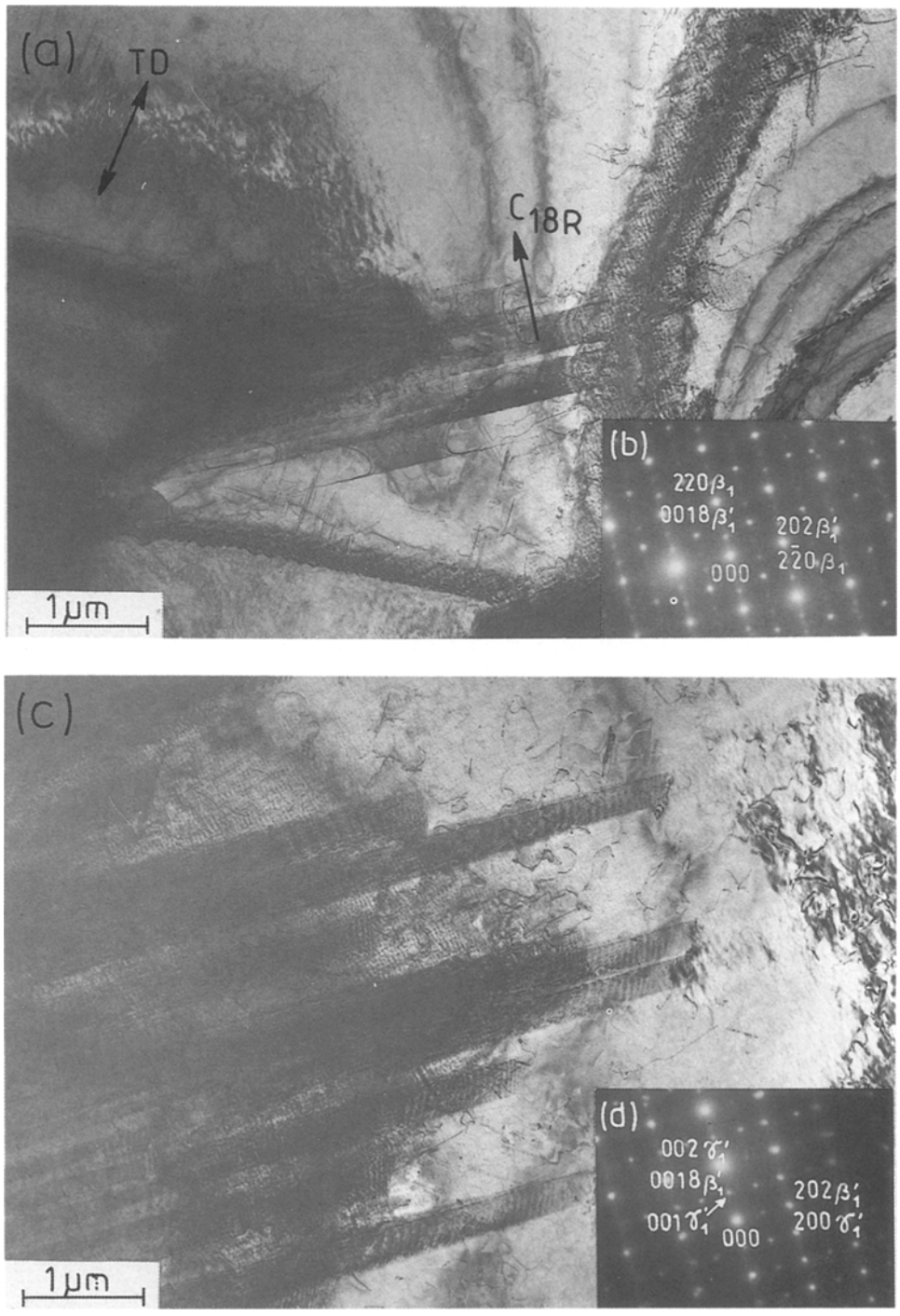

Figure 5 (a, c) Transmission electron micrographs showing propagation of β'_1 martensitic needles during *in situ* deformation in [1 0 0] direction: (b, d) corresponding electron diffraction pattern.

attributed either to the nonuniform stress field creating conditions to form β'_1 at this orientation, or to the small amount of β'_1 detectable only by means of transmission electron microscopy. In accordance with the difference in crystal structure the morphology of martensite formed at the [1 1 0] tensile axis has a different character than that at the [1 0 0] direction, i.e. separate needles of 18R structure are formed near large areas of 2H martensite. At [1 1 0] orientation a mixture of narrow needles (0.2–0.5 μm) of γ'_1 and β'_1 martensites is formed.

Another observation in the early stages of deformation is that very often c-axes of 18R or 2H structures are parallel or perpendicular to the direction of the needles which follow the $\langle 1\,1\,0\rangle\beta_1$ direction. During the growth of the needle its direction may change, however this is difficult to follow using transmission electron microscopy with a limited thin region. Therefore, the $(1\,\bar{5}\,\bar{5})$ and $(1\,\bar{3}\,\bar{3})$ habit planes observed in strained CuNiAl single crystals [9] using optical microscopy are confirmed in the present investigation, as $\langle 1\,1\,0\rangle$ direction lies within above mentioned planes.

Diffraction patterns from the β_1 phase show diffuse streaks in $\langle 1\,1\,0\rangle$ directions with no marked intensity increase in particular reciprocal lattice points. This effect does not change with the stress applied on the sample. Another diffraction effect, i.e. sideband reflections in the $\langle 1\,0\,0\rangle$ directions corresponding to the wavelength of modulations of a few tens of nanometres

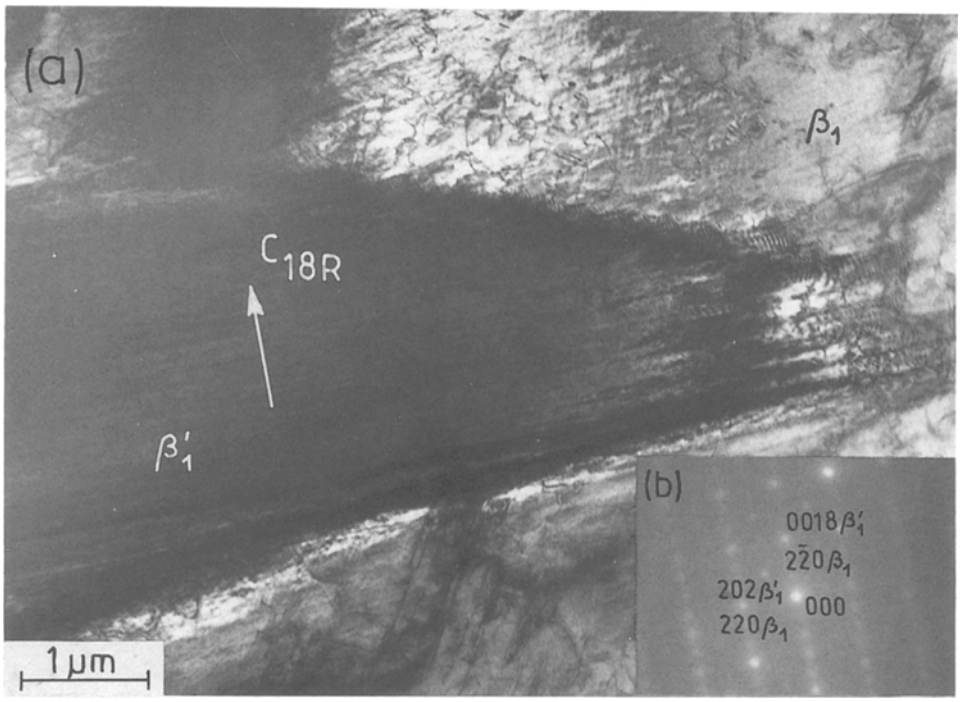

Figure 6 Transmission electron micrograph taken at maximum strain during the first cycle showing 18R martensite within β_1 matrix, (b) electron diffraction pattern from β'_1.

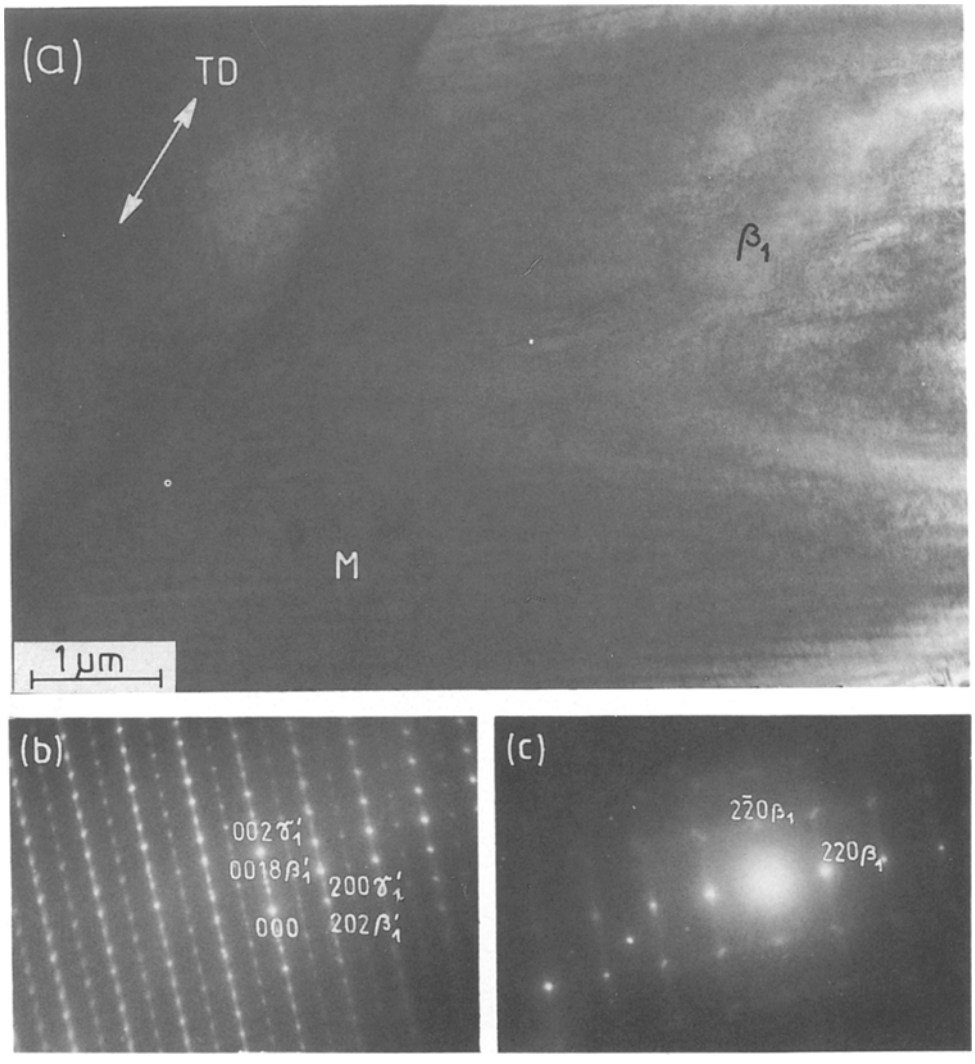

Figure 7 Transmission electron micrographs taken during the second cycle at the beginning of a stress release, (b) electron diffraction pattern from martensite, (c) electron diffraction pattern from β_1 matrix.

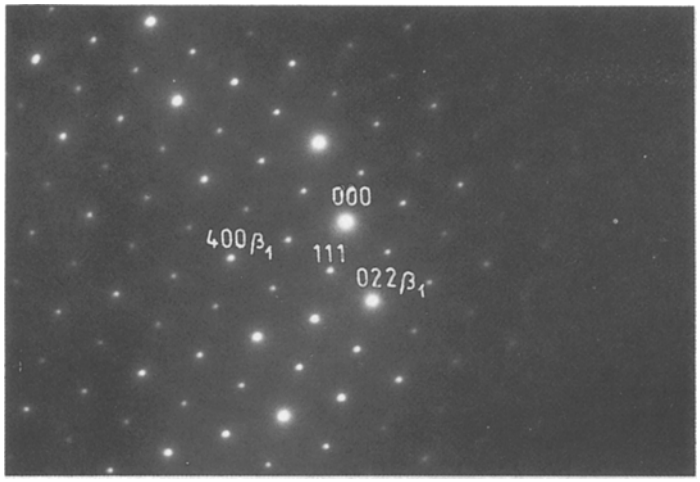

Figure 8 Electron diffraction pattern from β_1 phase taken during strain release in the second cycle.

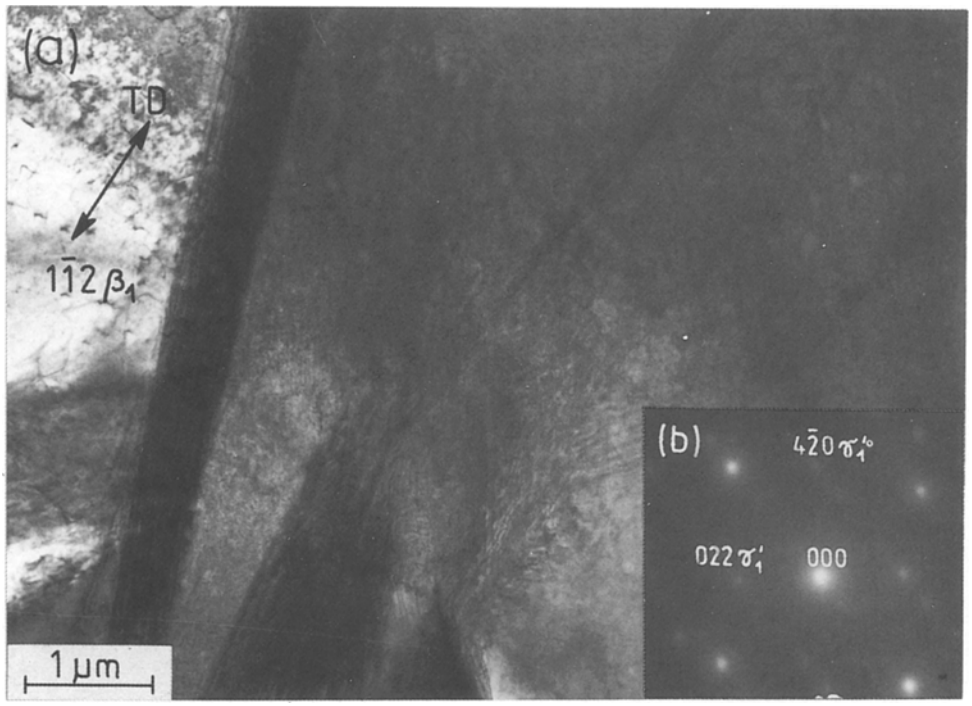

Figure 9 Transmission electron micrograph taken during strain release in the second cycle showing β_1/β_1' interphase, (b) diffraction pattern from γ_1' martensite.

Figure 10 Transmission electron micrograph taken during strain release in the second cycle showing two variants of martensite.

increases its intensity after the first stress induced transformation cycle, i.e. in places where a martensite recedes. This suggests that the elastic strain energy plays an important role in the generation of this effect and it is most probably related to the $\langle 1\,0\,1\rangle$ $\langle 1\,0\,\bar{1}\rangle$ static displacement waves as suggested by Robertson and Wayman [11] and van Tendeloo *et al.* [12]. Satellites appear in increased intensity at slightly tilted conditions from the ideal [0 0 1] orientation. This confirms the above mentioned explanation [11].

5. Conclusions

1. The HVEM *in situ* tensile deformation of CuAlFe monocrystalline samples of (0 0 1) foil plane orientation in the [1 1 0] direction causes the formation of γ_1' martensite. During the later stages of deformation narrow needles of β_1' nucleate in front of γ_1'.

2. During the deformation of samples of (0 0 1) foil plane orientation in [1 0 0] direction martensite forms as a mixture of narrow needles (0.2–0.5 μm in diameter) of γ_1' and β_1'.

3. The following crystallographic relationship between the parent phase and both types of martensite was observed: $[1\,0\,0]\beta_1 \| [1\,0\,1]\gamma_1'$ and $(0\,0\,1)\beta_1 \| (0\,1\,0)\gamma_1'$ and $(0\,0\,1)\beta_1 \| (0\,1\,0)\beta_1'$ and $[1\,1\,0]\beta_1 \| [0\,0\,1]\beta_1'$.

4. Under an applied stress the sideband reflections in $\langle 1\,0\,0\rangle$ directions appear at slightly tilted [0 0 1] orientation in increased intensity. This indicates the presence of $\langle 1\,0\,1\rangle$ $\langle 1\,0\,\bar{1}\rangle$ static displacement waves.

References

1. G. V. KURDIUMOV, *J. Tech. Fiz.* **18** (1948) 999.
2. G. V. KURDIUMOV and L. G KHANDROS, *Dokl. AN SSSR* **66** (1949) 211.
3. V. V. MARTYNOV and L. G. KHANDROS, *Znanie Ukr. SSR, Metalurgija, Kiev* 1980.
4. K. OTSUKA, H. SAKAMOTO and K. SHIMIZU, *Acta Metall.* **27** (1979) 585.
5. V. V. MARTYNOV, A. V. TKACHENKO and L. G. KHANDROS, *Dokl. AN SSSR* **242** (1979) 90.
6. V. V. MARTYNOV, K. ENAMI, A. V. TKACHENKO and L. G. KHANDROS, *Dokl. AN SSSR* **258** (III) (1981) 608.
7. J. DUTKIEWICZ, U. MESSERSCHMIDT, L. G. KHANDROS, V. V. MARTYNOV, F. APPEL and J. MORGIEL, *Scripta Metall.* **20** (1986) 813.
8. K. OTSUKA, C. M. WAYMAN, K. NAKAI, H. SAKAMOTO and K. SHIMIZU, *Acta Metall.* **24** (1976) 207.
9. H. SAKAMOTO and K. SHIMIZU, *Trans. JIM* **25** (1984) 845.
10. U. MESSERSCHMIDT and F. APPEL, *Ultramicroscopy* **1** (1976) 223.
11. I. M. ROBERTSON and C. M. WAYMAN, *Met. Trans.* **A15** (1984) 269.
12. G. VAN TENDELOO, M. CHANDRASEKARAN and F. C. LOVEY, *ibid.* **17A** (1986) 2153.

Received 25 July 1988
and accepted 4 January 1989